



PREPARATION, CHARACTERIZATION, AND *IN VITRO* ANTIBACTERIAL ACTIVITY OF Cu(II)-PYRAZINAMIDE COMPLEXES

**Galuh Wahyu Karti'a, Danar Purwonugroho, Arie Srihardyastutie, Yuniar Ponco
Prananto ***

*Department of Chemistry, Faculty of Mathematics and Natural Sciences, University of
Brawijaya, Malang, Indonesia*

ARTICLE INFO	ABSTRACT
<p>Keywords: <i>Anion dependent;</i> <i>antibacterial agent;</i> <i>copper complex;</i> <i>E. coli;</i> <i>S. aureus.</i></p> <p>Article History: <i>Received: 2024-04-24</i> <i>Accepted: 2024-06-21</i> <i>Published: 2024-07-13</i> <i>doi:10.20961/jkpk.v9i2.86189</i></p>	<p>Transition metal complexes, including <i>copper(II) complexes</i>, are being investigated as potential next-generation antibacterial agents. This study aims to prepare several <i>Cu(II)-pyrazinamide (Cu(II)-pza)</i> complexes using <i>Cu(II)</i> salts (acetate, chloride, nitrate, sulphate) through a direct mixing technique. Different <i>Cu(II)</i> salts are anticipated to yield distinct complexes, resulting in varied antibacterial properties. The <i>Cu(II)-pza</i> complexes were characterised using melting point analysis, infrared spectroscopy, and powder X-ray diffraction (XRD). Melting point analysis provides insights into the physical properties of the complexes. Infrared spectroscopy identifies functional groups and predicts chemical bonds within the complexes. Powder XRD analyses the characteristic diffraction patterns of the complexes. Experimental data reveal that the infrared spectra of all <i>Cu(II)-pza</i> complexes exhibit typical absorption bands of the pyrazinamide ligand (N-H, C=O, C-N, and C=N). Powder XRD analysis shows different diffraction patterns for each complex, indicating the formation of different compounds due to variations in anion and metal-ligand interactions, with the sulphate complex matching a previously reported complex. Melting point tests indicate the decomposition of the complexes within the range of 215–225 °C, except for the acetate complex, which decomposes at 275 °C. The antibacterial activities of these complexes against <i>S. aureus</i> and <i>E. coli</i> were examined <i>in vitro</i> based on inhibition zone diameter and MIC value. The sulphate, nitrate, and chloride complexes exhibit MIC values of 1,000 ppm and MBC values of 6,000 ppm, demonstrating better antibacterial activity against <i>S. aureus</i> than <i>E. coli</i>. These findings suggest the potential of <i>Cu(II)-pza</i> complexes as antibacterial agents. Further studies, such as crystal structure determination, are necessary to explore the possible mechanisms of antibacterial activity.</p>



©2024 The Authors. This open-access article is distributed under a (CC-BY-SA License)

*Corresponding Author Email: prananto@ub.ac.id

How to cite: G. W. Karti'a, D. Purwonugroho, A. Srihardyastutie, and Y. P. Prananto, "Preparation, characterisation, and *in vitro* antibacterial activity of Cu(II)-pyrazinamide complexes," *Jurnal Kimia dan Pendidikan Kimia (JKPK)*, vol. 9, no. 2, pp. 260-274, 2024. Available: <http://dx.doi.org/10.20961/jkpk.v9i1.86189>

INTRODUCTION

Climate change, driven by rapid industrial growth and high population density, is expected to create drier environmental conditions and increase air temperatures [1]. Higher temperatures can accelerate the

spread of bacterial pathogens, raising the risk of bacterial infections [2]. Antimicrobial resistance (AMR) has become a critical global issue, posing significant treatment challenges and escalating into a global health crisis. Pathogenic bacteria resistant to

antibiotics can survive and multiply in the presence of antibacterial agents, and the prevalence of this resistance is steadily rising worldwide, exacerbating the crisis [3].

The emergence of resistant strains of pathogenic bacteria is a major factor in the diminishing effectiveness of antibacterial agents. The Centers for Disease Control and Prevention (CDC) in the USA estimates that by 2050, if no new antibiotics are developed, multi-drug-resistant bacterial infections could cause 10 million deaths annually. To combat antibiotic-resistant bacteria, it is crucial to develop new antimicrobials targeting specific vulnerabilities in bacteria [4].

The World Health Organization (WHO) defines antimicrobial resistance as a condition where microorganisms no longer respond to antibiotics that were previously effective against them [5]. Reports indicate that nearly 75% of antimicrobials in clinical development are variations of existing molecules, which can lead to multiple resistances [6]. Therefore, innovative approaches are necessary for developing new antimicrobial agents.

The development of next-generation antibacterial agents is increasingly focusing on transition metal complexes. Unlike traditional antibiotics that target bacterial cell wall synthesis, protein synthesis, or DNA replication, transition metal complexes offer unique mechanisms of action. These include generating reactive oxygen species, disrupting metal homeostasis within bacterial cells, and interfering with essential enzyme functions [7].

Transition metal complexes exhibit various geometries that influence substitution

kinetics, charge, biological target lipophilicity, and their mode of action as antibacterial agents. The diversity in complex geometries enables the adoption of various structural configurations, allowing adjustments in shape and size to enhance interactions with biological targets and antimicrobial effectiveness. Variations in geometry also affect substitution kinetics, influencing how complexes interact and function within cells. Additionally, modifying the charge and lipophilicity of these complexes can improve their interaction with bacterial membranes, thereby increasing their effectiveness [8].

Transition metal complex compounds have been used to treat bacterial diseases for years [9]. The pharmacological activity of these drugs depends on the ligand, metal ion, and structure of the complex [10]. Certain metal ions can penetrate bacterial cell walls and deactivate enzymes, producing hydrogen peroxide to kill bacteria [7]. The effectiveness of complex compounds as antibacterial agents decreases in order based on their charge: cationic > neutral > anionic. Factors such as the ligand's chelation effect, the donor atom's nature, the metal complex's overall charge, the metal ion's nature, the reactivity of organic groups, and the geometric structure of the complex govern their antibacterial activity [11].

Transition metal complexes with ligands containing O and N donor atoms exhibit various configurations, structural stability, and responsiveness to various molecular environmental conditions, enhancing their potential as antibacterial agents. These ligands can bind to transition metals differently, forming octahedral,

tetrahedral, and square planar structures. This variability allows for specific adjustments to different bacterial targets, increasing the efficiency and spectrum of antibacterial activity. The central metal ion in these complexes serves as the active site for pharmacological agents [12].

Research on transition metal complexes as antibacterial candidates is receiving significant attention, with many complexes being tested for their potential antibacterial activity, including *Cu(II) complexes*.

Cu(II) complexes, particularly Cu (II), with pyrazinamide as the main ligand, hold significant importance in coordination chemistry due to their strong antibacterial potential [13]. These complexes have demonstrated promising results in inhibiting bacterial growth, making them central to developing new antibacterial agents. Free copper ions also harm bacteria and fungi [14]. They can cause cell membrane disruption, DNA damage, and inhibition of protein synthesis. Experimental studies indicate that antibacterials containing at least 55-70% copper metal can eliminate pathogenic microorganisms [15].

Pyrazinamide can form a five-membered ring through the nitrogen atom of the pyrazine ring and the oxygen atom of the carbonyl group, providing high stability to the complex, which enhances its antibacterial activity [13]. Pyrazinamide (pza), an amide derivative widely used for antituberculosis activity, has both bacteriostatic and bactericidal effects [16]. It can enter bacterial cells through diffusion. Once inside, the enzyme pyrazinamidase (PncA) activates

pyrazinamide to form pyrazinoic acid, which accumulates protons, causing the bacterial cytoplasm to become acidified and leading to cell membrane rupture [17]. Active pharmacophores in pyrazinamide compounds, such as amine groups, can inhibit bacterial growth and affect cell mitosis mechanisms [15].

The *Cu(II)-pyrazinamide* or *Cu(II)-pza* complex has numerous atom donors, enabling various coordination modes with metal ions, which enhances its interaction with bacterial cells and alters its antibacterial efficacy [12]. The complex features a C=N bond associated with better antimicrobial activity than those containing only C=C bonds [18].

In this study, four *Cu(II)-pyrazinamide* complexes were prepared, and three were tested against gram-positive bacteria (*S. aureus*) and gram-negative bacteria (*E. coli*). The effectiveness of the *Cu(II)-pyrazinamide* complex as an antibacterial agent is also discussed in comparison with free pyrazinamide and its salt precursor

METHODS

1. Material and Instrumentation

Lab-grade chemicals were used as received from the supplier (Merck Millipore), including $\text{Cu}(\text{CH}_3\text{COO})_2 \cdot 2\text{H}_2\text{O}$, $\text{CuCl}_2 \cdot 2\text{H}_2\text{O}$, $\text{Cu}(\text{NO}_3)_2 \cdot 3\text{H}_2\text{O}$, $\text{CuSO}_4 \cdot 5\text{H}_2\text{O}$, ethanol, pyrazinamide, and demineralised water. Additional materials included Mueller Hinton Broth (Himedia M391-500G), Mueller Hinton Agar (Himedia GRM026-500G), and McFarland standard 1—staphylococcus aureus ATCC 33591D-5 and Escherichia coli

ATCC 25922, supplied by CV. Wiyasa Mandiri (Malang, Indonesia) was used as the bacterial samples. Characterisation of the *Cu(II)*-pza complexes was performed using an infrared spectrophotometer (IRSpirit-T Shimadzu), powder-XRD (PANalytical X'pert3 Powder), and a melting point apparatus (InnoTech DMP800).

2. Synthesis of *Cu(II)*-Pyrazinamide Complexes

The synthesis of the complexes employed a *Cu(II)* molar ratio of 1:2 at room temperature. This ratio was based on previous research [19], which indicated that a 1:2 ratio of *Cu(II)* increases the likelihood of coordination with the copper(II) centre. For the synthesis, 0.487 mmol of each *Cu(II)* hydrous salt (nitrate = Nt, chloride = Cl, and acetate = Ac) was dissolved in 10 mL ethanol. In a separate vial, 0.975 mmol of pyrazinamide was dissolved in 10 mL ethanol. Both solutions were mixed in a beaker glass and stirred for 1 hour at 700 rpm, forming a precipitate. The precipitate was filtered, washed with ethanol, and oven-dried at 105 °C for 2 hours. For the sulphate (Su) complex, the procedure was identical to the other *Cu(II)* salts, except that an ethanol-water (1:1) mixture was used to dissolve the *Cu(II)*-sulphate at room temperature.

3. Characterization of the Complexes

The precipitated complexes were characterised using infrared spectroscopy (IR), melting point determination (MP), and powder X-ray diffraction (P-XRD). The IR analysis was conducted at 4000–400 cm⁻¹ using the KBr pellet method to confirm the presence of functional groups specific to the

anion and the pza ligand, focusing on the N-H, C=O, C-N, and C=N groups and compared with previous research [20]. The MP test was performed using an open capillary tube from 25 to 300°C at an increasing rate of 10 °C/min to evaluate the thermal stability and possible phase changes in the complexes. P-XRD analysis was conducted at room temperature with 2θ angles of 10–80° using Cu Kα = 1.54060 Å to identify the possible compounds and crystal structures of the complexes by comparing them with the powder diffraction patterns of other related compounds available in databases or journal articles. The degree of crystallinity (Xc) was calculated based on the convolution method [21], using Equation (1), where Xc is the degree of crystallinity, Ac is the area of the crystalline peak, and Aa is the area of the amorphous peak. Detailed calculations of the crystallinity degree were done using Origin 2022 software:

$$X_c = \frac{A_c}{(A_c + A_a)} \times 100 \quad (1)$$

4. Antibacterial activity

The Minimum Inhibitory Concentration (MIC) was used in this study to determine the lowest concentration of an antimicrobial agent that can inhibit bacterial growth after a 24-hour incubation period. The absence of bacterial colony growth recognises successful inhibition. *Staphylococcus aureus* and *Escherichia coli* were used in this study as they are pathogens that cause global pandemics with high mortality rates [22].

Each test tube was labelled 1-6, with tube 7 labelled K(+) as a positive control

containing pathogenic bacteria equivalent to McFarland turbidity standard 1, ensuring optimal bacterial growth conditions. Tube 8 was labelled K(-) as a negative control containing liquid Mueller Hinton broth media, serving as a baseline for the absence of antimicrobial activity. Tubes 1-6 were filled with 1 mL of nutrient broth liquid media. A 1 mL complex solution with concentrations of 1,000, 2,000, 3,000, 4,000, 5,000, and 6,000 ppm was taken using a micropipette, placed in separate vials, and mixed homogeneously. The absorbance was measured using a spectrophotometer at 600 nm. Concentrations below 1,000 ppm did not show any inhibition, whereas concentrations above 6,000 ppm were difficult to achieve since the complex was not fully dissolved.

The solutions were incubated at 37°C for 24 hours. MIC was assessed through visual turbidity. If the turbidity in each tube remained equal to or higher than the K(+), it suggests that the bacteria were still growing. If the solution in the treatment tube was clearer or similar to the K(-), it suggests that bacterial growth was inhibited, indicating the MIC. The absorbance of the treatment sample was measured using a UV-Vis spectrophotometer (600 nm).

The MIC assay, Minimum Bactericidal Concentration (MBC), was characterised by spreading samples on Mueller-Hinton agar plates from the wells that exhibited no evident growth. Plates were incubated at 37 °C for 24 hours to assess bactericidal activity. This step confirmed whether the MIC assay's concentration that inhibited bacterial growth was bactericidal.

Antibacterial activity was evaluated using the Kirby-Bauer standard disk diffusion assay for the zone of inhibition (ZOI) and the standard well diffusion assay for MIC. The antibacterial activity of *Cu(II)*-pyrazinamide complexes was investigated in vitro against *Escherichia coli* (Gram-negative) and *Staphylococcus aureus* (Gram-positive). These pathogens were grown in Mueller Hinton broth at 10⁶ CFU/mL for 18-24 hours. Bacterial colonies from culture bottles were poured into Petri dishes containing nutrient agar. Solutions of pyrazinamide, CuCl₂·2H₂O, Cu(NO₃)₂·3H₂O, CuSO₄·5H₂O, and the complexes (chloride, nitrate, and sulphate) with concentrations of 1,000 ppm and 6,000 ppm were prepared. Blank discs were dipped into the samples and mounted on Petri dishes according to the standard disc diffusion assay (Kirby-Bauer). The disks were incubated for 24 hours at 37°C until a clear zone formed. The average of three replicates was used to represent each sample. Pyrazinamide and solvent (demineralised water) were used as positive and negative controls.

RESULTS AND DISCUSSION

1. Synthesis of *Cu(II)*-Pyrazinamide complexes

All reaction series produced precipitates of varying colours, indicating that different anions of *Cu(II)* salts resulted in different complexes: light blue (sulphate), bright blue (nitrate), green (chloride), and grey (acetate) (Figure 1). These colour differences suggest that each reaction produced distinct complex compounds, with the anion of the salt playing a significant role in the composition of the final product.

In transition metal complexes, the d orbitals experience splitting into t_{2g} (low energy) and, e.g. (high energy) orbitals [23]. This splitting creates an energy gap corresponding to energy transitions and absorption in the visible light region, leading to different colours depending on the energy levels [24].



Figure 1

. Photos of the synthesised Cu(II)-pyrazinamide complexes from different Cu(II) salt sources.

When an anion coordinates to a Cu(II) metal centre (acting as a strong field ligand), it causes electronic transitions in the d orbitals, changing the electron configuration. If the anion acts only as a counter ion or a weak field ligand, the electron transition may not occur. This results in different energy gaps between t_{2g} and, e.g., corresponding to different wavelengths of visible light [23]. Therefore, different anions in the Cu(II) complex, either as counter ions or ligands, result in varying colours [25].

The yield of each reaction series cannot be accurately calculated because the complex's chemical formula and molecular weight still need to be determined.

Crystallography analysis, such as single-crystal XRD, could provide this information but requires single-crystal samples, which were not obtained in this study. Although the complex may precipitate in a high mass, the yield (%) might be low if it has a high molecular weight. Calculating the yield based on the mass (mg) of the complex obtained from 1 mmol of Cu(II) salt (mg/mmol), the results are as follows, from low to high: Su (207.4) < Ac (244.4) < Nt (248.5) < Cl (266.9). The Su complex had the lowest yield due to the different solvents used; the water in the ethanol-water mixture (1:1) might dissolve some of the complex formed, unlike the other reactions using ethanol alone. These yields are relatively low, partly due to the low initial concentrations of Cu(II) salts and pza used in this study ([Cu] = 0.00487 mM; [pza] = 0.00975 mM). It is predicted that higher concentrations would result in higher yields.

The MP test was conducted to study the complexes' thermal stability and potential phase changes. It also aimed to determine whether the products differed by comparing their melting points (Table 1). The chloride, nitrate, and sulphate complexes all decomposed (turned black) at slightly different temperatures. The acetate complex decomposed at a higher temperature (275 °C), indicating better thermal stability than the other complexes. This suggests that the acetate complex may have a polymeric structure or a coordination environment around the metal ion with bridging ligands or a polynuclear complex.

Although the nitrate and chloride complexes had nearly similar decomposition temperatures, they are different compounds

due to their distinct colours. The sulphate complex produced in this study decomposed at a lower temperature than the identical complex previously reported [19], which was 260 °C (without any drying procedure before testing). This discrepancy may be due to the sulfate complex being dried in an oven at 105

°C for 2 hours before testing, potentially causing structural defects. No colour change was observed during the test, indicating no phase change occurred as the complex was heated.

Table 1. Physical properties of the complex from each reaction series

Reaction Code	Cu(II) salts	Cu(II) (mmol)	Pza (mmol)	Average Mass (mg)	Colour of Complex	Decompose (°C)
Su	Sulphate	0.4875	0.9750	101	Light blue	229
Nt	Nitrate	0.4875	0.9750	121	Blue	218
Cl	Chloride	0.4875	0.9750	130	Green	220
Ac	Acetate	0.4875	0.9750	119	Grey	275

2. Characterization of complexes

Infrared spectroscopy analysis was conducted to identify the functional groups in the product. These functional groups confirm the presence or absence of the pyrazinamide ligand and any anions involved in the complex. The analysis helps determine the

formation of the *Cu(II)*-pyrazinamide complex by examining changes or shifts in absorption peaks and comparing the data with the free pyrazinamide ligand and related complexes [26]. The infrared spectra of the complexes, compared to the free pyrazinamide ligand, are presented in **Figure 2**, with detailed information in **Table 2**.

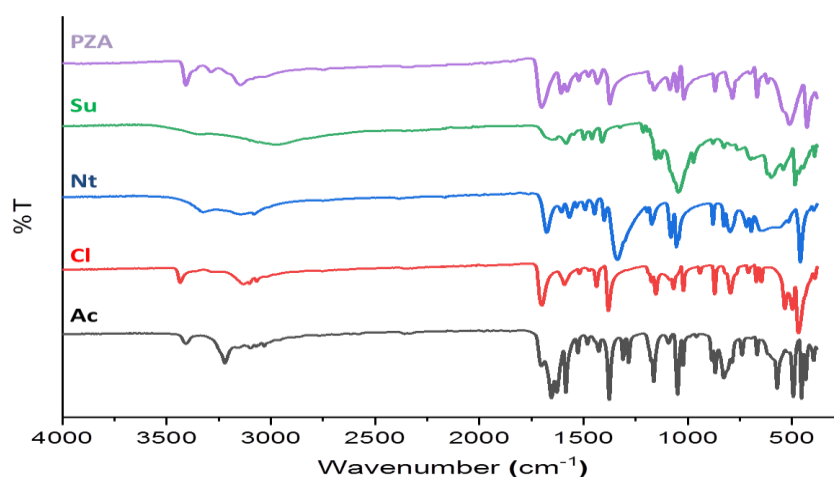


Figure 2. Infrared spectra of pyrazinamide and Cu(II) complexes

Analysis of the infrared spectra confirmed that *Cu(II)*-pyrazinamide complexes were formed from all *Cu(II)* salts. This is supported by the appearance of two bands in

the ~3400 and ~3200 cm⁻¹ region with medium intensity, corresponding to the asymmetric and symmetric stretching vibrations of the -NH₂ group. Absorption

bands of C-N vibrations shifted to higher wavelengths, indicating that coordination bonds were formed at the pyrazine nitrogen between the pyrazinamide ligands and the metal centre [27].

The carbonyl vibrational peak also shifted to a higher wavenumber in the acetate complex. This suggests that the acetate anion and the central atom might form a coordination bond, or the acetate likely acts as a ligand in the complex. The difference between asymmetric and symmetric ($\Delta\nu$) frequency of C=O is 74 cm^{-1} , indicating that the acetate group forms a symmetrical bridging coordination pattern, which may correspond to a paddle wheel structure around the metal centre. This has also been reported in the

crystal structure of $[\text{Cu}_2(\text{niacinamide})_2(\text{acetate})_4]$ [28]. These carboxylate groups can be assumed to have a symmetric bridging conformation, where both oxygen atoms of the two carboxylate groups are coordinated to one copper ion. Therefore, the coordination environment around the metal center in the acetate complex is expected to adopt a paddle-wheel structure.

In the sulphate complex, new peaks appear around 1045 cm^{-1} , corresponding to the vibrational stretch of the sulphate group, indicating the presence of sulphate anions. The presence of nitrate in the nitrate complex is confirmed by an intense peak around 1300 cm^{-1} .

Table 2. Infrared data (cm^{-1}) of pyrazinamide and Cu(II)-pyrazinamide complexes.

Pza	Su	Nt	Cl	Ac	Interpretation
3407	3341	3324	3435	3408	$-\text{NH}_2$ (asymmetric)
3285	3200	3225	3278	3220	$-\text{NH}_2$ (symmetric)
1701	1648	1677	1700	1702	C=O (asymmetric)
1607	1583	1608	1591	1628, 1654	C=O (symmetric)
1373	1411	1406	1380	1376	C-N _{pyrazine}
1578	1582	1567	1520	1584	C=C _{pyrazine}
520	541	516	533	570	C=N _{pyrazine}
-	1045	-	-	-	sulphate
-	-	1337	-	-	nitrate

The powder diffraction patterns of the complexes are shown in Figure 3. These patterns are compared with those of a related complex previously published [19]. The four complexes obtained in this study exhibit significantly different diffraction patterns, confirming that they are distinct compounds with different crystal systems. The melting point data and infrared spectra analysis also support this. Diffraction patterns reflect the arrangement and spacing between atoms in a crystal lattice. Different anions (acetate,

chloride, nitrate, and sulphate) coordinate to Cu(II), forming different geometries and coordination environments, resulting in various crystal structures. Variations in crystal structures influence the antibacterial properties of the complexes. The distinct coordination environments affect the complexes' overall stability, solubility, and polarity, which govern their ability to interact with bacterial cells. As a result, each complex produces a unique powder diffraction pattern.

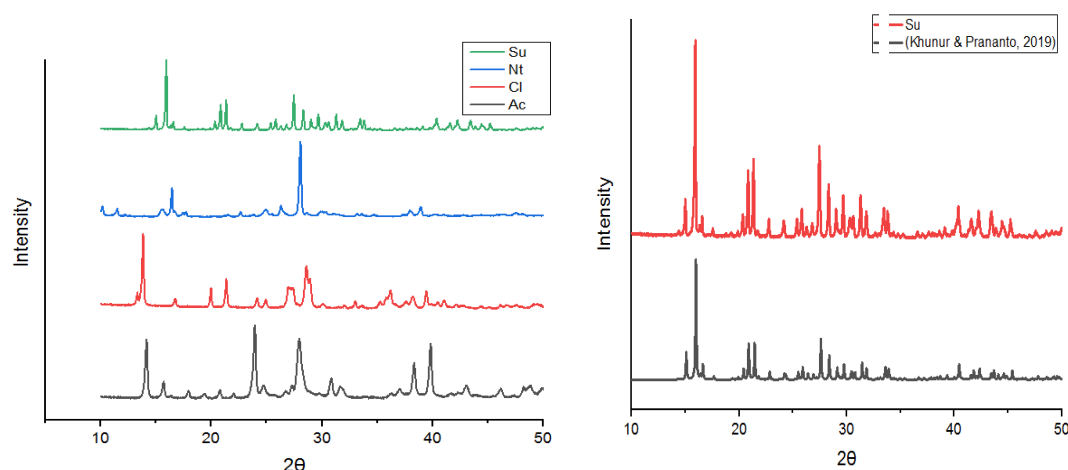


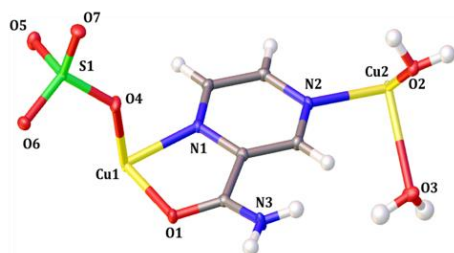
Figure 3. Powder diffraction patterns of Cu(II)-pyrazinamide complexes obtained from this study (left) and compared to published work (right)

Different Cu(II) salt anions resulted in different structures and compounds. The structures of *Cu(II)*-pyrazinamide complexes are influenced by the anion of the *Cu(II)* salt used in the reaction, where the anion may act as a ligand or a free counter ion. Degrees of crystallinity of the complexes vary as follows: 36%, 38%, 48%, and 54% for the nitrate, chloride, acetate, and sulphate complexes, respectively. These differences arise from each reaction series forming distinct compounds. Specifically, the sulphate complex precipitated from a different solvent mixture (ethanol-water 1:1), affecting the crystallisation growth rate. Compared to similar studies [19], this study resulted in complexes with lower crystallinity degrees, attributed to the different synthesis methods. The direct mixing technique used in this study leads to a lower crystallinity degree than the layering technique due to the high nucleation rate caused by fast contact between the metal ion and the ligand. However, the direct mixing technique significantly reduces time consumption compared to the layered technique.

The sulphate complex obtained in this study has an identical powder diffraction pattern (Figure 3) to that of a previous study [19], confirming that the sulphate complex is $[Cu(pza)(SO_4)(H_2O)_2]_n$, where the sulphate acts as a ligand and the complex forms a 1D chain [19]. The asymmetric unit of the complex is shown in Figure 4.

The acetate complex of *Cu(II)*-pyrazinamide is predicted to be $[Cu_2(niacinamide)_2(acetate)_4]$ based on the IR spectra and calculation of the difference between asymmetric and symmetric ($\Delta\nu$) frequency of C=O, as reported by [28]. Determining the structures of the chloride and nitrate complexes is not possible at this stage due to the formation of low-quality single crystals for single-crystal XRD analysis. Both complexes are predicted to adopt octahedral geometry with the probability of forming discrete or polymeric structures, as the pyrazine ring of pza can bridge two neighbouring metal ions. A Jahn-Teller effect may also be observed in these *Cu(II)* complexes, a common feature of *Cu(II)*-complexes [19] [29].

The presence of the anion likely governs the structure and crystal packing of the chloride and nitrate complexes. Both nitrate and chloride may act as a ligand or as a free counter ion in their complex; therefore, several proposed formulas of the complex



are possible, e.g., $[\text{Cu}(\text{pza})_2(\text{H}_2\text{O})_2(\text{Cl})_2]$, $[\text{Cu}(\text{pza})_2(\text{H}_2\text{O})_2]\text{Cl}_2$, $[\text{Cu}(\text{pza})_2(\text{H}_2\text{O})_2(\text{NO}_3)_2]$, or $[\text{Cu}(\text{pza})_2(\text{H}_2\text{O})_2](\text{NO}_3)_2$. The data currently available is insufficient to determine which formula is the most accurate prediction.

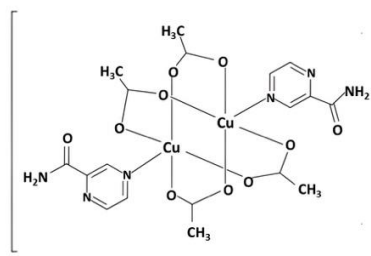


Figure 4. The asymmetric unit of the sulphate complex (left), which is identical to the $[\text{Cu}(\text{pza})(\text{SO}_4)(\text{H}_2\text{O})_2]_n$ reported by [19], and predicted structure of the acetate complex (right: $[\text{Cu}_2(\text{CH}_3\text{COO})_4(\text{pza})_2]$) [23].

3. Antibacterial Activity

The MIC test, using the dilution method with Nutrient Broth as the incubation medium for 24 hours, showed that the complexes (sulphate, nitrate, and chloride) at concentrations of 1,000 ppm to 6,000 ppm had varying levels of solution clarity against *S. aureus* and *E. coli* compared to the solvent control (K(-)) and untreated bacterial suspension (K(+)). At 1,000 ppm, all three complexes demonstrated effectiveness as antibacterial agents, with solutions appearing clearer than K(+) and resembling the clarity of K(-). At 6,000 ppm, the solutions maintained clarity close to their initial colour and were similar to K(-).

A recent study [30] reported a MIC of 2500 ppm for the *Cu(II)*-niacinamide complex, suggesting that the *Cu(II)*-pza complexes synthesised in this study are more effective (MIC = 1000 ppm) than the *Cu(II)*-niacinamide complex. This indicates that *Cu(II)*-pza shows better potency in inhibiting bacterial growth at lower concentrations.

Determining the MBC involved transferring the liquid cultures used in MIC testing onto new agar plates. MBC was found at 6,000 ppm for the three complexes tested against *E. coli* and *S. aureus* cultures, indicating that higher concentrations are needed to kill the bacteria completely.

The sulphate, nitrate, and chloride complexes were tested against bacterial strains using the Kirby-Bauer well diffusion test method, with complex concentrations based on MIC and MBC procedures. Antimicrobial activity was assessed by determining MIC or MBC in vitro after anaerobic incubation. Various complex concentrations were tested, with results presented in Table 3. The zone of inhibition (Zoi) differed in colour from other areas where bacteria grew, as it was free of bacterial colonies. Among the three complexes, the chloride complex exhibited the strongest inhibitory activity against both bacteria.

Table 3. Zone of Inhibition (Zol)

Compounds	Zone of inhibition diameter \pm STD			
	<i>S. aureus</i> (1,000 ppm)	<i>E. coli</i> (1,000 ppm)	<i>S. aureus</i> (6,000 ppm)	<i>E. coli</i> (6,000 ppm)
Su complex	13 \pm 1.7	10 \pm 0.82	18 \pm 1.63	15 \pm 0.94
Nt complex	10 \pm 0.94	11 \pm 1.25	19 \pm 1.25	16 \pm 0.82
Cl complex	12 \pm 0.82	9 \pm 0.47	21 \pm 1.61	18 \pm 1.41
Pyrazinamide	10 \pm 0.47	10 \pm 0.94	13 \pm 1.41	12 \pm 0.94
CuSO ₄ ·5H ₂ O	9 \pm 0.82	8 \pm 0.47	10 \pm 0.82	10 \pm 0.47
Cu(NO ₃) ₂ ·3H ₂ O	9 \pm 0.47	7 \pm 0.00	9 \pm 0.47	8 \pm 0.47
CuCl ₂ ·2H ₂ O	10 \pm 0.82	8 \pm 0.47	11 \pm 0.47	10 \pm 0.82
Solvent (H ₂ O)	0 \pm 0	0 \pm 0	0 \pm 0	0 \pm 0

*STD: Standard of Deviation

This study shows that all synthesised *Cu(II)*-pyrazinamide complexes exhibited greater antibacterial activity than the initial *Cu(II)* salts and free pyrazinamide. The coordination between the ligand and the metal ion can balance the positive charge with the donor atom or group, reducing the polarity of the metal ion [31]. This process can make the core metal atom more lipophilic, enhancing penetration and lipid layer damage in microorganisms [10]. The study also reveals that all three *Cu(II)*-pza complexes showed similar levels of activity against the same bacteria at 6,000 ppm, with insignificant differences in inhibition zones among the three complexes: approximately 14.06–19.41 mm (weak to moderate) for *E. coli* and 16.37–22.61 mm (medium to strong) for *S. aureus*.

XRD analysis indicates that the sulphate complex forms a neutral complex, with pza as a bridging ligand. As a result, the polar groups in pza mainly coordinate to the metal center, reducing the activity of the sulphate complex compared to the nitrate and chloride complexes. The insignificant differences in activity between the nitrate and chloride complexes and the sulphate complex suggest that the nitrate and chloride

complexes may also form neutral compounds. However, specific interactions between nitrate or chloride ions and the metal center may differ, potentially affecting antibacterial activity differently.

The sulphate complex showed lower antibacterial properties than the nitrate and chloride complexes, likely due to its higher polarity index, making it more difficult to diffuse into the nonpolar bacterial lipid membranes. Molecules with higher polarity tend to interact more strongly with water molecules and other polar substances, reducing their ability to penetrate non-polar bacterial membranes [32]. The Zol value of the chloride complex indicates better antibacterial activity compared to similar complexes reported [13], with 14 mm for *S. aureus* and 16 mm for *E. coli*. Furthermore, the sulphate and chloride complexes showed longer Zol diameters than identical complexes reported [33] using niacinamide instead of pza, with the sulphate complex giving 7 mm for *E. coli* and 0 mm for *S. aureus*. In comparison, the chloride complex gave 0 mm for *E. coli* and 8 mm for *S. aureus*. Compared to commercially available antibiotics such as Streptomycin, which had inhibition zones of 22.00 ± 2.83 for *E. coli* and

21.00 ± 1.41 for *S. aureus* [34], the *Cu(II)*-pyrazinamide complexes were less effective. The three complexes generally showed better antibacterial activity toward *S. aureus* (16.37–22.61 mm) than *E. coli* (14.06–19.41 mm). This difference is because *E. coli* is a gram-negative bacterium with a more complex and thicker cell surface structure. The cell surface of *E. coli* consists of peptidoglycan cell walls, plasmatic membranes, and outer lipid bilayer structures characteristic of gram-negative bacteria. The outer layer acts as a selective barrier due to the high negative charge provided by lipopolysaccharides and its selectivity level from porins. Certain antibiotics can destroy gram-positive bacteria more than gram-negative bacteria [35].

The antibacterial mechanism of complex compounds involves the degradation of metal ions, facilitated by the release of metal ions from the ligand. The ease of metal ion release determines the complex compound's ability as an antibacterial agent. Released metal ions can alter the bacterial cell environment, disrupting ion balance and damaging ion channels and membrane integrity. Cell membrane rupture and cytoplasmic leakage can lead to bacterial death, resulting from structural damage to bacterial cells due to the attack by antibacterial agents. Additionally, organic ligands in complex compounds exhibit antibacterial effects through continuous release, synergising with the metal ions released by the complex compound [36].

CONCLUSION

Different *Cu(II)* salts lead to the formation of *Cu(II)*-pza complexes with varying colours and compositions due to the distinct roles of the anions in the complex formation. Infrared spectroscopy's characterisation showed typical absorption bands of the pyrazinamide ligand (N-H, C=O, C-N, and C=N). P-XRD analysis of each complex revealed different powder diffraction patterns and degrees of crystallinity. Melting point tests indicated decomposition of the complexes in the range of 218–229 °C, except for the acetate complex, which decomposed at 275 °C.

The antibacterial activity of the sulphate, nitrate, and chloride complexes against *S. aureus* and *E. coli* showed that the complexes have a MIC of 1,000 ppm and an MBC of 6,000 ppm. The three complexes demonstrated better antibacterial activity against *S. aureus* than *E. coli*. These results suggest the potential of *Cu(II)*-pza complexes as candidates for antibacterial agents. Further studies, such as crystal structure determination, are needed to explore the possible mechanisms of their antibacterial activity.

ACKNOWLEDGMENT

This study was part of a fast-track program in the Department of Chemistry at Brawijaya University. The authors acknowledge the Postgraduate Program of the Chemistry Department, Brawijaya University, and the microbiology laboratory at LRT (formerly LSIH), Brawijaya University.

SUPPLEMENTARY

Supplementary data related to this study's antibacterial tests and synthesis procedures can be accessed in Supplementary 1.

REFERENCES

- [1] N. C. Handayani, A. Kusuma, R. Purwanto, R. E. Prasetya, and A. Budiman, "Pengembangan Agen Potensi Pengembangan Agen Antibakteri dari Senyawa Kompleks Logam Transisi di Indonesia," *The Indonesian Green Technology Journal*, vol. 10, no. 1, pp. 9-20, 2021.
- [2] R. S. Hellberg and E. Chu, "Effects of climate change on the persistence and dispersal of foodborne bacterial pathogens in the outdoor environment: A review," *Crit. Rev. Microbiol.*, vol. 42, no. 4, pp. 548–572, 2016. doi: [10.3109/1040841X.2014.967385](https://doi.org/10.3109/1040841X.2014.967385).
- [3] T. Li, Y. Wang, X. Zhang, J. Chen, and L. Sun, "Bacterial resistance to antibacterial agents: Mechanisms, control strategies, and implications for global health," *Sci. Total Environ.*, vol. 860, p. 160148, 2023. doi: [10.1016/j.scitotenv.2022.160148](https://doi.org/10.1016/j.scitotenv.2022.160148).
- [4] N. A. Church and J. L. McKillip, "Antibiotic resistance crisis: challenges and imperatives," *Biologia (Bratisl.)*, vol. 76, no. 5, pp. 1535–1550, 2021. doi: [10.2478/s11756-021-00707-5](https://doi.org/10.2478/s11756-021-00707-5).
- [5] World Health Organization, "Global Action Plan for antimicrobial resistance," vol. 105, no. 5, p. 70780, 2015.
- [6] World Health Organization, "Antibacterial agents in clinical development: an analysis of the antibacterial clinical development," 2019. [Online]. Available: <https://www.who.int/publications/i/item/9789240000193>.
- [7] M. Rizzotto, "Metal Complexes as Antimicrobial Agents," *A Search Antibact. Agents*, vol. 10, p. 45651, 2012.
- [8] S. N. Sovari and F. Zobi, "Recent Studies on the Antimicrobial Activity of Transition Metal Complexes of Groups 6–12," *Chem.*, vol. 2, no. 2, pp. 418–452, 2020. doi: [10.3390/chemistry2020025](https://doi.org/10.3390/chemistry2020025).
- [9] M. Claudel, C. Ragonnaud, S. Yousfi, A. Choisy, and R. Gaertner, "New Antimicrobial Strategies Based on Metal Complexes," *Chemistry*, vol. 2, no. 4, pp. 849–899, 2020. doi: [10.3390/chemistry2040067](https://doi.org/10.3390/chemistry2040067).
- [10] G. Borthagaray, L. Quintana, F. Brocal, and L. A. Rodríguez, "Infectious Diseases and Epidemiology Essential Transition Metal Ion Complexation as a Strategy to Improve the Antimicrobial Activity of Organic Drugs," *J. Infect. Dis. Epidemiol.*, vol. 2, no. 2, p. 14, 2016.
- [11] S. Mittapally, R. Taranum, and S. Parveen, "Metal ions as antibacterial agents," *Journal of Drug Delivery and Therapeutics*, vol. 8, pp. 411–419, 2018. doi: [10.22270/jddt.v8i6.2018](https://doi.org/10.22270/jddt.v8i6.2018).
- [12] J. Ara Shampa, "Physiochemical and Antibacterial Activity Investigation on Noble Schiff Base Cu(II) Complex," *Am. J. Heterocycl. Chem.*, vol. 3, no. 4, p. 37, 2017.
- [13] A. E. Ali, M. El-Ghamry, M. H. Saker, and A. K. Hussein, "Spectral, thermal studies and biological activity of pyrazinamide complexes," *Heliyon*, vol. 5, no. 11, p. e02912, 2019. doi: [10.1016/j.heliyon.2019.e02912](https://doi.org/10.1016/j.heliyon.2019.e02912).
- [14] Q. C. Burandt, B. L. Knierim, S. Sundström, and F. Jacquet, "Further Limitations of Synthetic Fungicide Use and Expansion of Organic Agriculture in Europe Will Increase the Environmental and Health Risks of Chemical Crop Protection Caused by

- Copper-Containing Fungicides," *Environ. Toxicol. Chem.*, vol. 43, no. 1, pp. 19–30, 2024. doi: [10.1002/etc.4995](https://doi.org/10.1002/etc.4995).
- [15] M. Vincent, L. Duval, R. Hartemann, J. Noury, and P. Perrin, "Antimicrobial applications of copper," *Int. J. Hyg. Environ. Health*, vol. 219, no. 7, pp. 585–591, 2016. doi: [10.1016/j.ijheh.2016.07.003](https://doi.org/10.1016/j.ijheh.2016.07.003).
- [16] M. S. Khan, R. Farooq, M. A. Baig, and H. Shahid, "Computational investigation of pyrazinamide drugs and its transition metal complexes using a DFT approach," *J. Comput. Chem.*, vol. 45, no. 10, pp. 622–632, 2024. doi: [10.1002/jcc.26563](https://doi.org/10.1002/jcc.26563).
- [17] E. A. Lamont and N. A. Dillon, "The Bewildering Antitubercular Action of Pyrazinamide," *Microbiology and Molecular Biology Reviews*, vol. 84, no. 2, pp. 1–15, 2020. doi: [10.1128/MMBR.00034-19](https://doi.org/10.1128/MMBR.00034-19).
- [18] N. Raman and R. Jeyamurugan, "Synthesis, characterization, and DNA interaction of mononuclear copper(II) and zinc(II) complexes having a hard-soft NS donor ligand," *J. Coord. Chem.*, vol. 62, no. 14, pp. 2375–2387, 2009. doi: [10.1080/00958970902932390](https://doi.org/10.1080/00958970902932390).
- [19] M. M. Khunur and Y. P. Prananto, "Structural analysis of polymeric copper(ii)-pyrazinamide complexes prepared from two different copper(II) salts," *IOP Conf. Ser. Mater. Sci. Eng.*, vol. 546, no. 6, 2019. doi: [10.1088/1757-899X/546/6/062015](https://doi.org/10.1088/1757-899X/546/6/062015).
- [20] M. Ahmed, S. H. Naz, M. H. Siddiqui, M. Tahir, and A. S. Farooqi, "Synthesis, characterization and anticancer activity of isonicotinylhydrazide metal complexes," *J. Chem. Soc. Pakistan*, vol. 41, no. 1, pp. 113–121, 2019. [Online]. Available: <https://jcspp.org.pk/issueDetail.aspx?aid=90>.
- [21] A. H. Rafika, M. H. Tarafder, K. Mahmood, and S. I. A. Razak, "Effect of drying temperature and drying time on the crystallinity degree of Zn(II)-tartrate complex," *Kuwait J. Sci.*, vol. 50, no. 4, pp. 596–601, 2023. doi: [10.48129/kjs.v50i4.11354](https://doi.org/10.48129/kjs.v50i4.11354).
- [22] S. Tsuzuki, T. Hayashi, K. Muranaka, M. Kamata, T. Iwasaki, and K. Nishimura, "National trend of bloodstream infection attributable deaths caused by *Staphylococcus aureus* and *Escherichia coli* in Japan," *J. Infect. Chemother.*, vol. 26, no. 4, pp. 367–371, 2020. doi: [10.1016/j.jiac.2019.10.014](https://doi.org/10.1016/j.jiac.2019.10.014).
- [23] A. S. Coia, G. Müller, F. Körner, and H. W. Lang, "Exploring the Role of Transition Metal Complexes in Artistic Coloration through a Bottom-Up Scientific Approach," *J. Cult. Herit.*, 2024. doi: [10.1016/j.culher.2023.05.004](https://doi.org/10.1016/j.culher.2023.05.004).
- [24] M. Manimohan, S. Karthikeyan, M. Ponnuswamy, and M. S. Suriyanarayanan, "Biologically active Co (II), Cu (II), Zn (II) centered water soluble novel isoniazid grafted O-carboxymethyl chitosan Schiff base ligand metal complexes: Synthesis, spectral characterisation, and DNA nuclease activity," *International Journal of Biological Macromolecules*, vol. 163, pp. 801-816, 2020. doi: [10.1016/j.ijbiomac.2020.06.118](https://doi.org/10.1016/j.ijbiomac.2020.06.118).
- [25] W. H. Turner, "Optical Absorption Spectra of Iron in The Rock-Forming Silicates: a Discussion," *American Mineralogist: Journal of Earth and Planetary Materials*, vol. 52, no. 3-4, pp. 553-555, 1967. doi: [10.2138/am-1967-3-428](https://doi.org/10.2138/am-1967-3-428).
- [26] Y. Chen, Z. Lu, and X. Zhang, "Applications of Micro-Fourier Transform Infrared Spectroscopy (FTIR) in the Geological Sciences — A

- Review," *Appl. Spectrosc. Rev.*, vol. 50, no. 4, pp. 30223–30250, 2015. doi:[10.1080/05704928.2015.1115401](https://doi.org/10.1080/05704928.2015.1115401).
- [27] M. Ali, S. G. Tushar, A. K. Najji, and R. Ahmad, "Design, synthesis and antitubercular evaluation of novel series of pyrazinecarboxamide metal complexes," *Iran. J. Pharm. Res.*, vol. 17, no. 1, pp. 93–99, 2018. doi: [10.22037/ijpr.2018.2124](https://doi.org/10.22037/ijpr.2018.2124).
- [28] B. Kozlevčar, B. Zupančič, M. Hren, and B. Šket, "Complexes of copper (II) acetate with nicotinamide: preparation, characterization and fungicidal activity; crystal structures of [Cu₂(O₂CCH₃)₄(nia)] and [Cu₂(O₂CCH₃)₄(nia)₂]," *Polyhedron*, vol. 18, no. 5, pp. 755–762, 1999. doi: [10.1016/S0277-5387\(98\)00354-7](https://doi.org/10.1016/S0277-5387(98)00354-7).
- [29] O. Kristiansson, "Bis(pyrazine-2-carboxamide)bis(trifluoromethanesulfonate)copper(II) monohydrate," *Acta Crystallogr. Sect. E Struct. Reports Online*, vol. 58, no. 3, pp. m130–m132, 2002. doi: [10.1107/S1600536802006196](https://doi.org/10.1107/S1600536802006196).
- [30] N. C. Handayani, I. K. Dewi, M. Surya, and S. Utami, "Synthesis, Characterization, and Antibacterial Activity of Anion-Depended Cu (II)-Niacinamide Complexes," *The Indonesian Green Technology Journal*, vol. 11, no. 2, pp. 1–12, 2020. doi: [10.1016/j.kjs.2023.02.008](https://doi.org/10.1016/j.kjs.2023.02.008).
- [31] P. Ghanghas, S. K. Ghanghas, and A. S. Thakur, "Coordination metal complexes with Schiff bases: Useful pharmacophores with comprehensive biological applications," *Inorg. Chem. Commun.*, vol. 130, p. 108710, 2021. doi: [10.1016/j.inoche.2021.108710](https://doi.org/10.1016/j.inoche.2021.108710).
- [32] N. C. S. Mykytczuk, P. L. Trevors, and E. B. Twiss, "Fluorescence polarization in studies of bacterial cytoplasmic membrane fluidity under environmental stress," *Prog. Biophys. Mol. Biol.*, vol. 95, no. 1–3, pp. 60–82, 2007. doi: [10.1016/j.pbiomolbio.2007.03.001](https://doi.org/10.1016/j.pbiomolbio.2007.03.001).
- [33] S. Njobdi, N. T. J. Jebin, and A. J. Ishaku, "Antibacterial Activity of Zingiber officinale on Escherichia coli and Staphylococcus aureus," *J. Adv. Biol. Biotechnol.*, vol. 19, no. 1, pp. 1–8, 2018. doi: [10.9734/jabb/2018/39840](https://doi.org/10.9734/jabb/2018/39840).
- [34] G. Kumaravel, R. R. Mounika, S. Harini, and K. K. Nithya, "Bioorganic Chemistry Exploiting the biological efficacy of benzimidazole based Schiff base complexes with L-Histidine as a co-ligand: Combined molecular docking, DNA interaction, antimicrobial and cytotoxic studies," *Bioorg. Chem.*, vol. 77, pp. 269–279, 2018. doi: [10.1016/j.bioorg.2018.01.022](https://doi.org/10.1016/j.bioorg.2018.01.022).
- [35] M. Shen, L. Li, T. Hu, and J. Fang, "Antibacterial applications of metal–organic frameworks and their composites," *Compr. Rev. Food Sci. Food Saf.*, vol. 19, no. 4, pp. 1397–1419, 2020. doi: [10.1111/1541-4337.12558](https://doi.org/10.1111/1541-4337.12558).